Electronic Supplementary Material (ESI) for RSC Advances.

Supporting information

Development of cellulose-based polymeric structures using dual functional ionic liquids

Joana Galamba[a], Vítor D. Alves[b], Noémi Jordão[a]*, Luísa A. Neves[a]*

[a] *LAQV-REQUIMTE, Chemistry Department, Nova School of Science and Technology | FCT NOVA, Universidade NOVA de Lisboa, Campus de Caparica, 2829-516 Caparica, Portugal*
[b] *LEAF, Linking Landscape, Environment, Agriculture and Food, Instituto Superior de Agronomia, Universidade de Lisboa, Tapada da Ajuda, 1349-017 Lisboa, Portugal*

Table of Contents

1. Synthesis and structural characterization of ILs

[BE][OAc] Yellow viscous liquid (51.54 g, 98%). ^{1}H NMR (400.13 MHz, DMSO-d6, 25ºC) δ = 7.58 (d, J = 7.16 Hz 2H), 7.54 – 7.47 (m, 3H), 7.26 (d, J = 8.04 Hz, 2H), 6.83 (d, J = 8.00 Hz, 2H), 4.68-4.64 (m, 2H), 4.15-4.11 (m, 2H), 4.07-4.05 (m, 2H), 3.95-3.69 (m, 2H, overlap with H_2O signal), 3.62-3.54 (m, 2H), 3.03 (s, 6H), 1.70-1.64 (m, 2H), 1.63-1.57 (m, 3H), 1.33-1.23 (m, 6H), 0.70-0.62 (m, 9H) ppm. ^{13}C NMR (APT) (100.61 MHz, DMSO-d6, 25ºC) δ = 172.6, 156.0, 141.5, 133.2, 130.2, 128.8, 128.2, 126.9, 113.6, 68.8, 67.4, 66.6, 63.9, 62.5, 56.3, 49.7, 37.6, 32.0, 31.5, 25.4 ppm. Anal. Calcd (%) for $C_{29}H_{45}NO_4.3.7H_2O$: C 64.70, H 9.81, N 2.60; found: C 64.54, H 9.85, N 2.69.

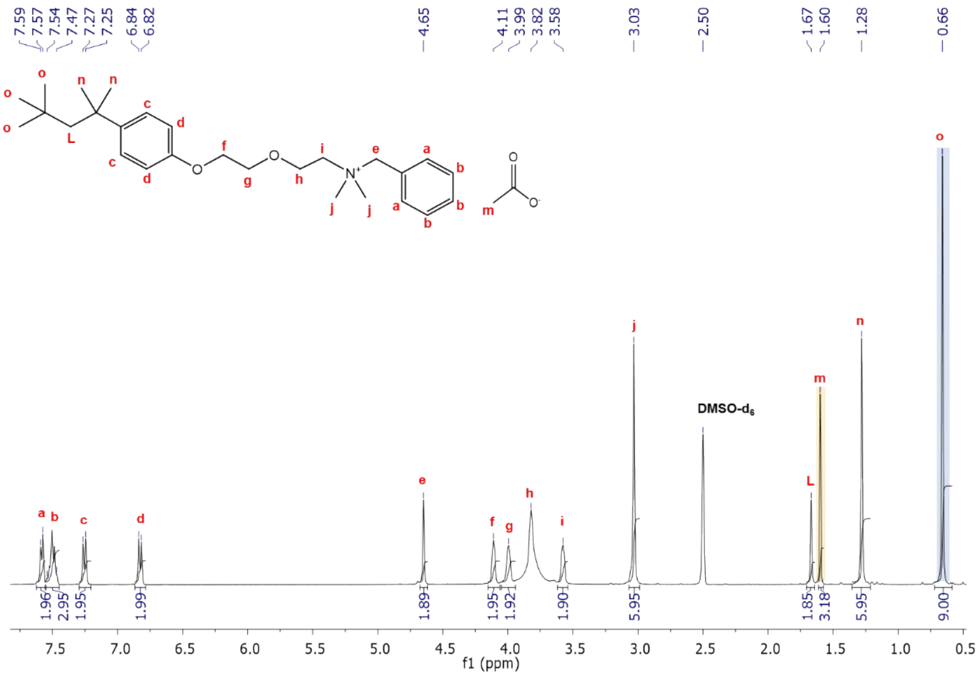

SI-Figure 1. ^{1}H NMR (400.13 MHz, DMSO-d6, 25ºC) of [BE][OAc].

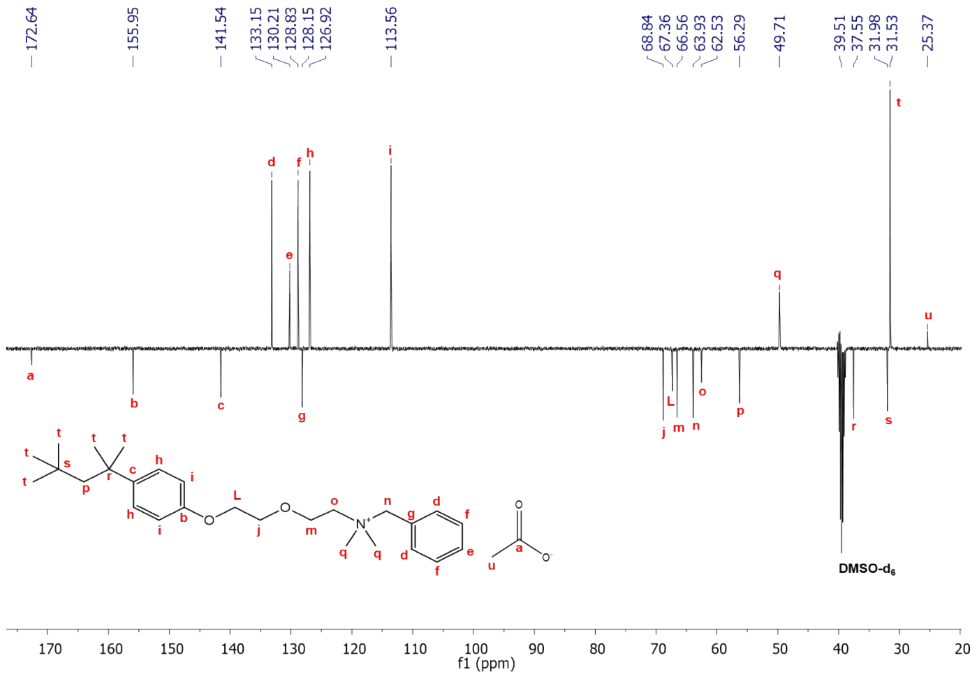

SI-Figure 2. ^{13}C NMR APT (100.61 MHz, DMSO-d6, 25ºC) of [BE][OAc].

[BE][OPr]: Yellow viscous liquid (53.11 g, 98%). [1]H NMR (400.13 MHz, DMSO-d6, 25ºC) δ = 7.58 (d, J = 7.24 Hz, 2H), 7.54 – 7.47 (m, 3H), 7.25 (d, J = 7.92 Hz, 2H), 6.83 (d, J = 7.84 Hz, 2H), 4.68-4.64 (m, 2H), 4.15-4.08 (m, 2H), 4.04-3.95 (m, 2H), 3.87-3.78 (m, 2H), 3.66-3.46 (m, 2H, overlap with H_2O signal), 3.03 (s, 6H), 1.83 – 1.78 (m, 2H), 1.71-1.63 (m, 2H), 1.28 (s, 6H), 0.87 (t, J = 7.56 Hz, 3H), 0.69-0.62 (s, 9H) ppm. [13]C NMR (APT) (100.61 MHz, DMSO-d6, 25ºC) δ = 175.9, 156.0, 141.6, 133.2, 130.2, 128.9, 128.2, 126.9, 113.6, 68.9, 67.4, 66.6, 64.0, 62.5, 56.3, 49.7, 37.6, 32.0, 31.5, 31.4, 11.4 ppm. Anal. Calcd (%) for $C_{30}H_{47}NO_4.4.2H_2O$: C 64.19, H 9.95, N 2.50; found: C 64.15, H 9.94; N 2.58.

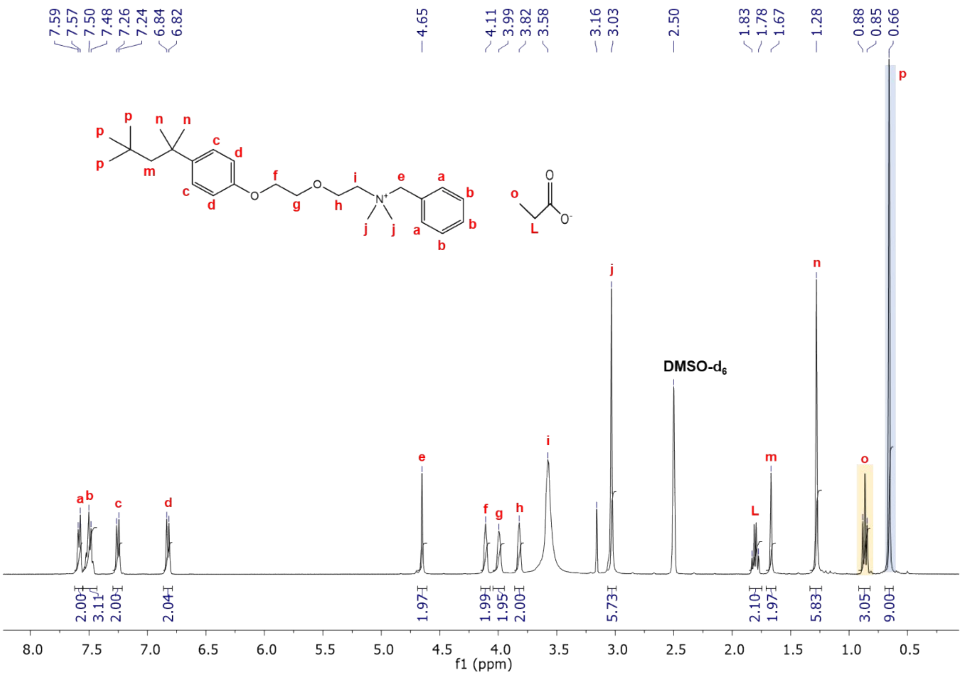

SI-Figure 3. [1]H NMR (400.13 MHz, DMSO-d6, 25ºC) of [BE][OPr].

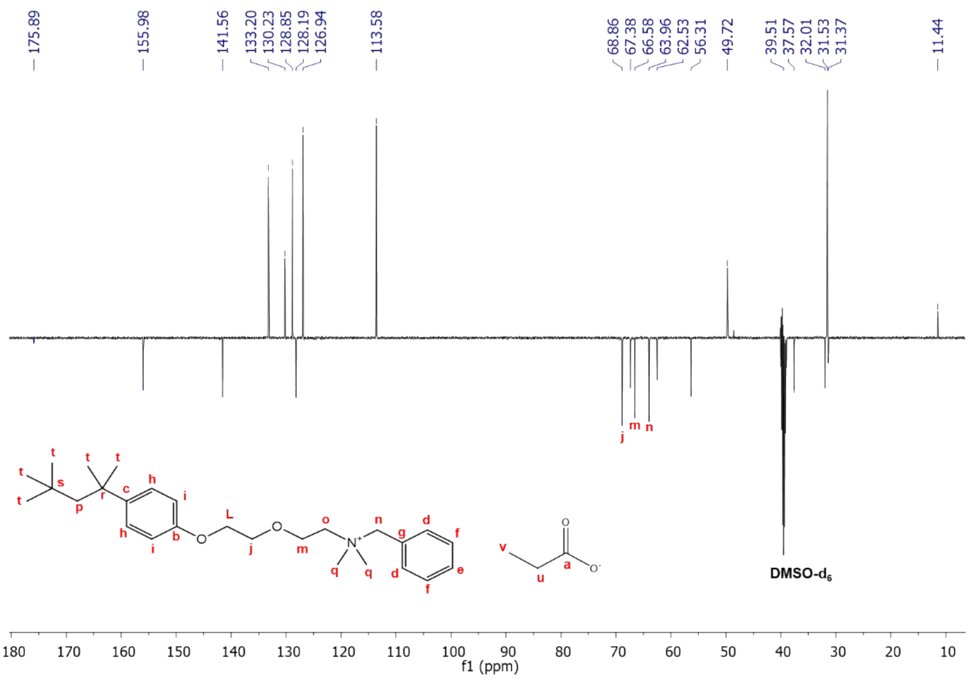

SI-Figure 4. [13]C NMR APT (100.61 MHz, DMSO-d6, 25ºC) of [BE][OPr].

[BE][OHex]: Yellow viscous liquid in quantitative yield (58.89 g, 100%). [1]H NMR (400.13 MHz, DMSO-d6, 25ºC) δ = 7.59 (d, J = 7.2Hz, 2H) 7.50 – 7.46 (m, 3H), 7.25 (d, J = 7.96 Hz, 2H), 6.83 (d, J = 7.88 Hz, 2H), 4.69-4.62 (m, 2H), 4.15-4.07 (m, 2H), 4.04-3.96 (m, 2H), 3.86-3.79 (m, 2H), 3.71-3.47 (m, 2H, overlap with H_2O signal), 3.04 (s, 6H), 1.81 (t, J = 7.38 Hz, 2H), 1.72-1.61 (m, 2H), 1.42 – 1.35 (m, 2H), 1.28 (s, 6H), 1.24 – 1.15 (m, 4H), 0.83 (t, J = 6.72 Hz, 3H), 0.71-0.62 (m, 9H) ppm. [13]C NMR (APT) (100.61 MHz, DMSO-d6, 25ºC) δ = 175.3, 156.0, 141.6, 133.2, 130.2, 128.8, 128.2, 126.9, 113.6, 68.9, 67.4, 66.6, 64.0, 62.5, 56.3, 49.7, 37.6, 32.0, 31.8, 31.6, 26.3, 22.2, 14.1 ppm. Anal. Calcd (%) for $C_{33}H_{53}NO_4.4H_2O$: C 66.08, H 10.25, N 2.34; found: C 65.93, H 10.40; N 2.42.

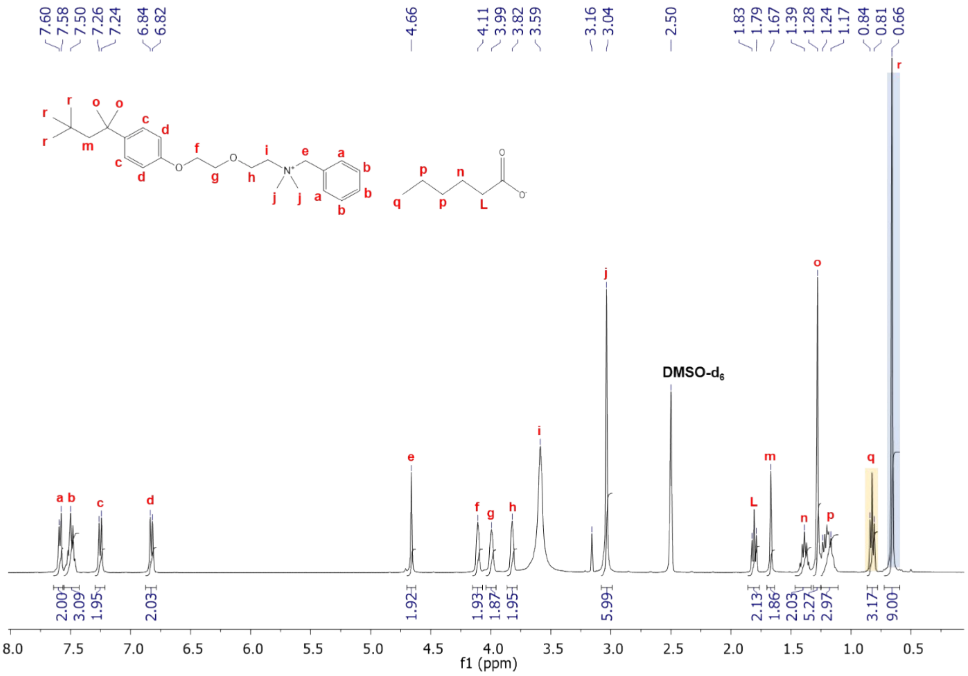

SI-Figure 5. [1]H NMR (400.13 MHz, DMSO-d6, 25ºC) of [BE][OHex].

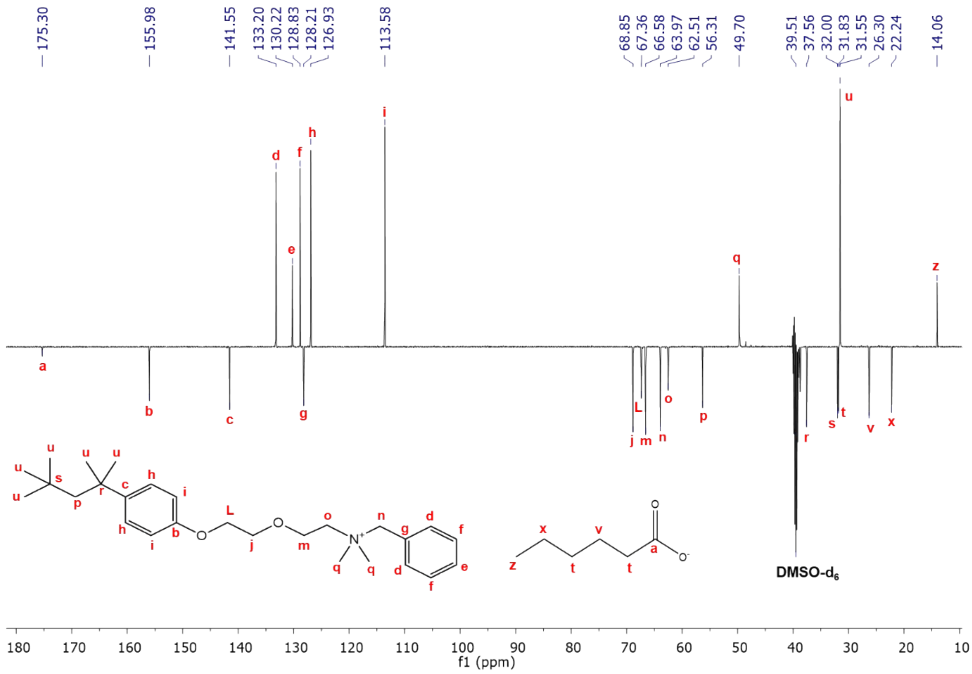

SI-Figure 6. [13]C NMR APT (100.61 MHz, DMSO-d6, 25ºC) of [BE][OHex].

[DDA][OAc]: Pale orange viscous liquid in quantitative yield (47.43 g, 100%). [1]H NMR (400.13 MHz, D_2O, 25ºC) δ = 3.28 – 3.12 (m, 4H), 3.04 (s, 6H), 1.85 (s, 3H), 1.70-1.51 (m, 4H), 1.40 – 1.14 (d, 28H), 0.91 – 0.89 (m, 6H) ppm. [13]C NMR (APT) (100.61 MHz, DMSO-d6, 25ºC) δ = 180.1, 61.6, 52.0, 32.0, 29.6, 29.4, 29.1, 28.7, 25.5, 22.8, 22.6, 21.8, 13.8 ppm. Anal. Calcd (%) for $C_{24}H_{51}NO_2.3.5H_2O$): C 64.22, H 13.07, N 3.12; found: C 64.24 H 13.03 N 3.12.

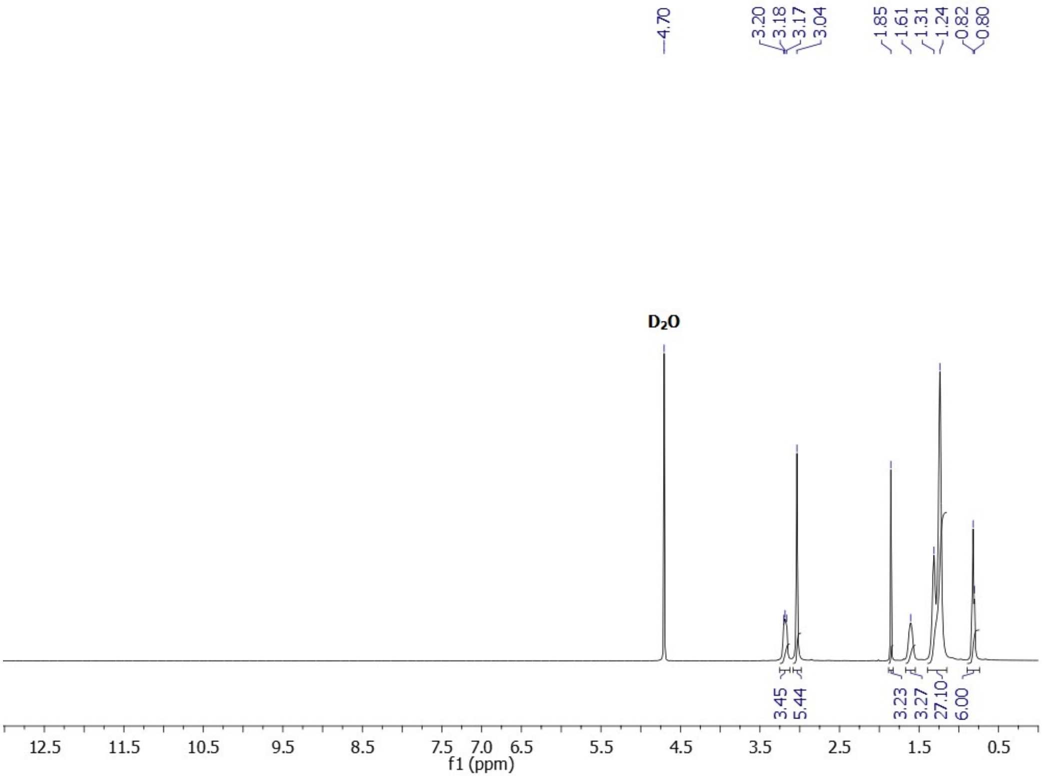

SI-Figure 7. [1]H NMR (400.13 MHz, D_2O, 25ºC) of [DDA][OAc].

SI-Figure 8. [13]C NMR APT (100.61 MHz, D_2O, 25ºC) of [DDA][OAc].

[DDA][OPr]: Pale orange viscous liquid in quantitative yield (49.16 g, 100%). [1]H NMR (400.13 MHz, D_2O, 25ºC) δ = 3.32 – 3.21 (m, 4H), 3.12 (s, 6H), 2.27 – 2.16 (m, 2H), 1.76-1.61 (m, 4H), 1.47 – 1.21 (d, 28H), 1.07 (t, J = 7.60 Hz, 3H), 0.96 – 0.83 (m, 6H) ppm. [13]C NMR (ATP) (100.61 MHz, DMSO-d6, 25ºC) δ = 183.2, 61.6, 52.1 32.0, 30.1, 29.6, 29.4, 29.1, 28.7, 25.6, 22.6, 21.9, 13.8, 9.9 ppm. Anal. Calcd (%) for $C_{25}H_{53}NO_2.3.2H_2O$: C 65.66 H 13.09 C3.06 found: C 65.66 H 13.11 N 3.05.

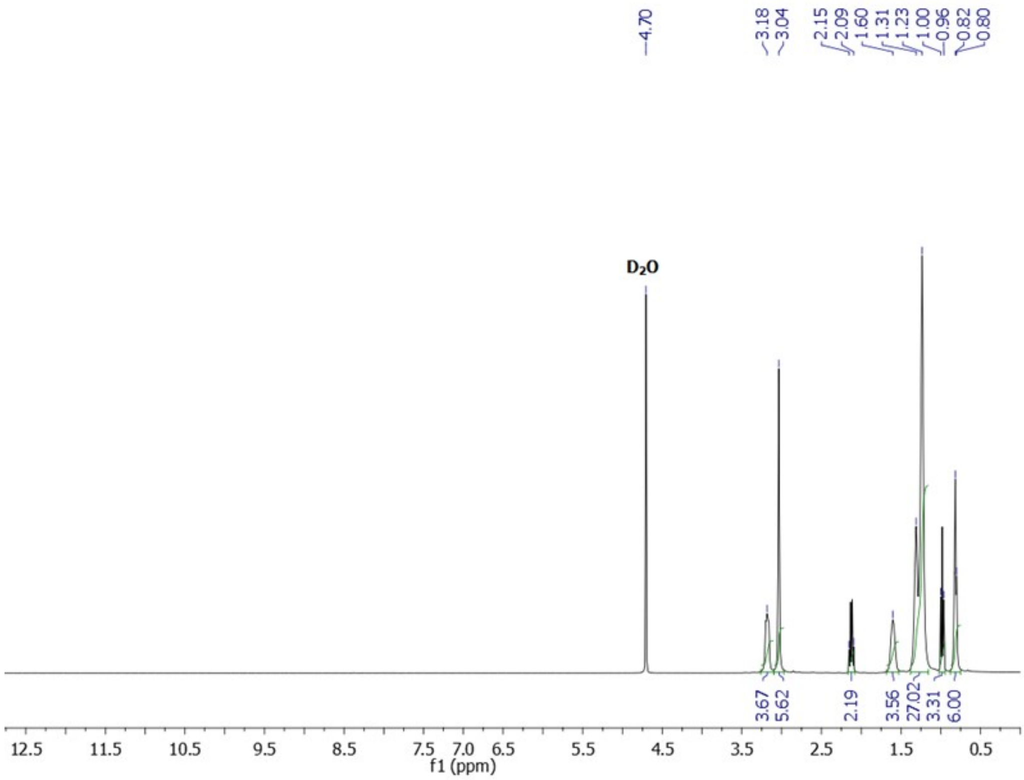

SI-Figure 9. [1]H NMR (400.13 MHz, D_2O, 25ºC) of [DDA][OPr].

SI-Figure 10. [13]C NMR APT (100.61 MHz, D_2O, 25ºC) of [DDA][OPr].

[DDA][OHex]: Pale orange viscous liquid in quantitative yield (54.34 g, 100%). ^{1}H NMR (400.13 MHz, DMSO-d6, 25ºC) δ = 3.29 – 3.18 (m, 4H), 3.00 (s, 6H), 1.77 (t, J = 7.38 Hz, 2H), 1.69-1.55 (m, 4H), 1.43 – 1.13 (m, 2H anion + 28H cation + 4H anion), 0.91 – 0.80 (m, 6H cation + 3H anion) ppm. ^{13}C NMR (APT) (100.61 MHz, DMSO-d6, 25 ºC) δ = 174.9, 62.7, 49.9, 31.9, 31.3, 28.9, 28.8, 28.7, 28.5, 26.4, 25.8, 22.3, 22.1, 21.7, 14.1, 13.9 ppm. Anal. Calcd (%) for $C_{28}H_{59}NO_2.3.5H_2O$: C 66.62, H13.18, N2.77; found C 66.68, H 13.48, N 2.77.

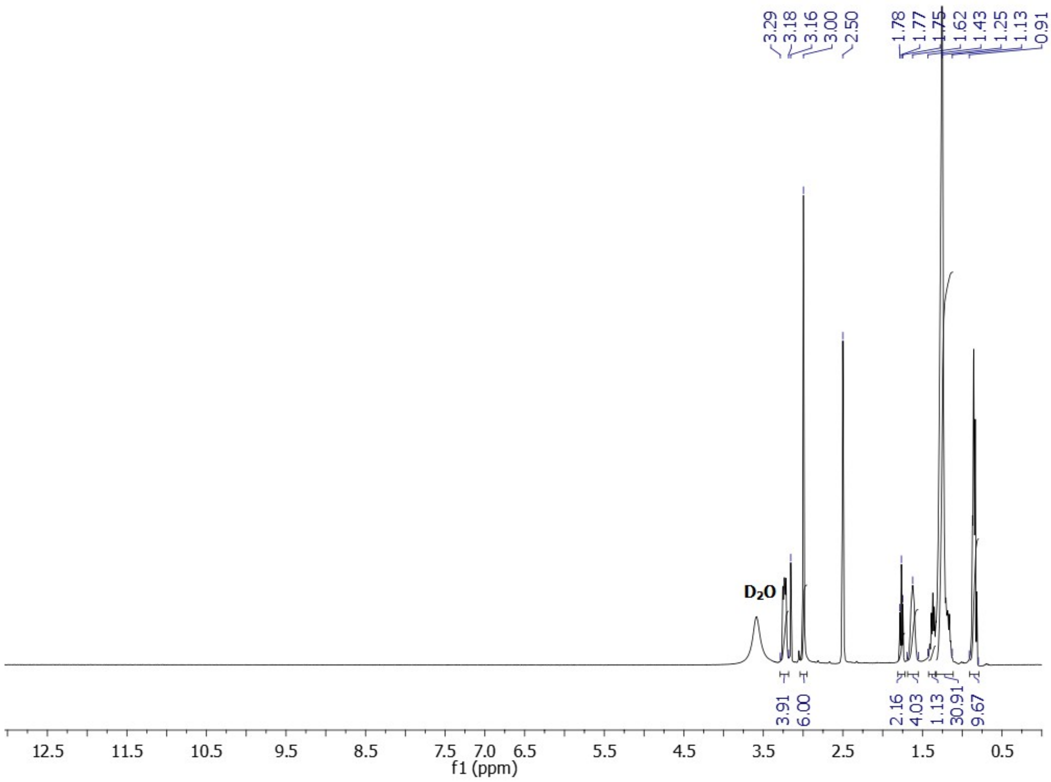

SI-Figure 11. ^{1}H NMR (400.13 MHz, DMSO-d6, 25ºC) of [BE][OHex].

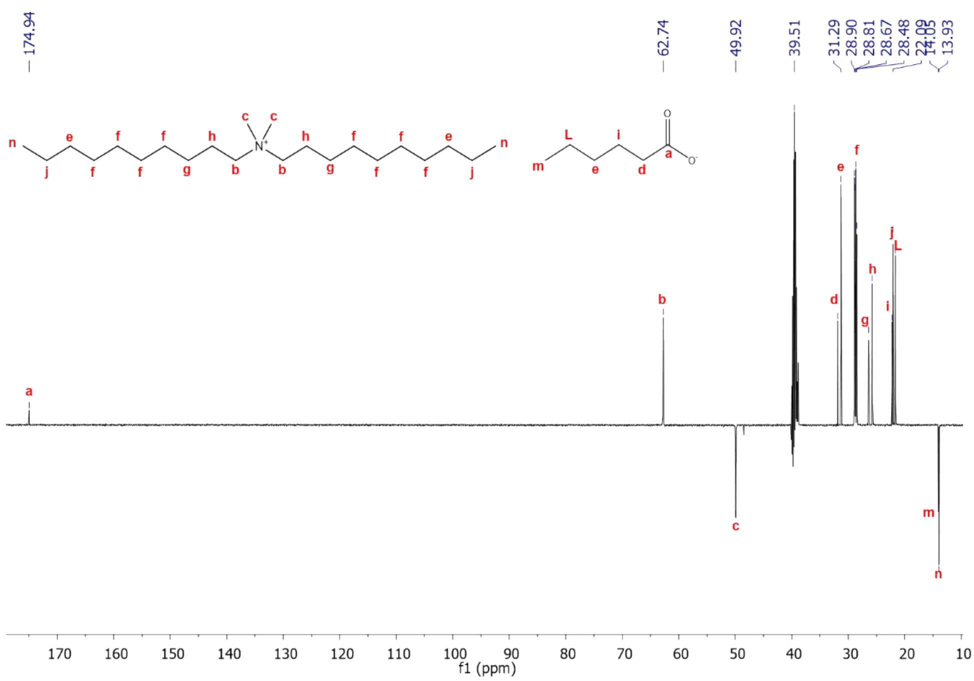

SI-Figure 12. ^{13}C NMR APT (100.61 MHz, DMSO-d6, 25ºC) of [BE][OHex].

2. ATR-FTIR spectroscopy

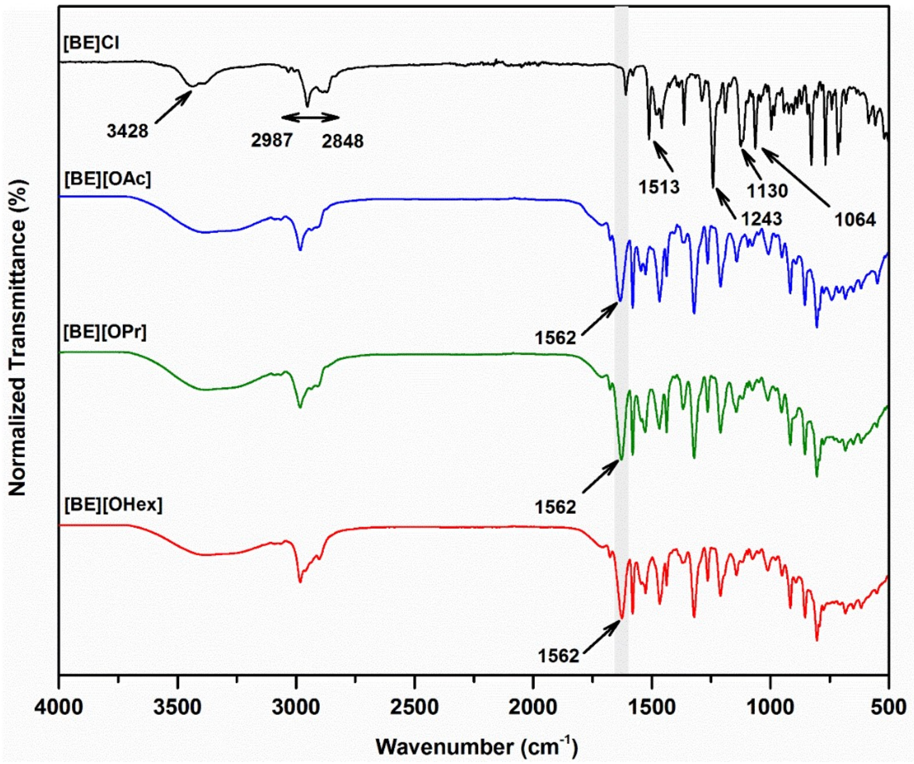

SI-Figure 13. FTIR-ATR spectra of [BE]Cl and [BE] based-ILs.

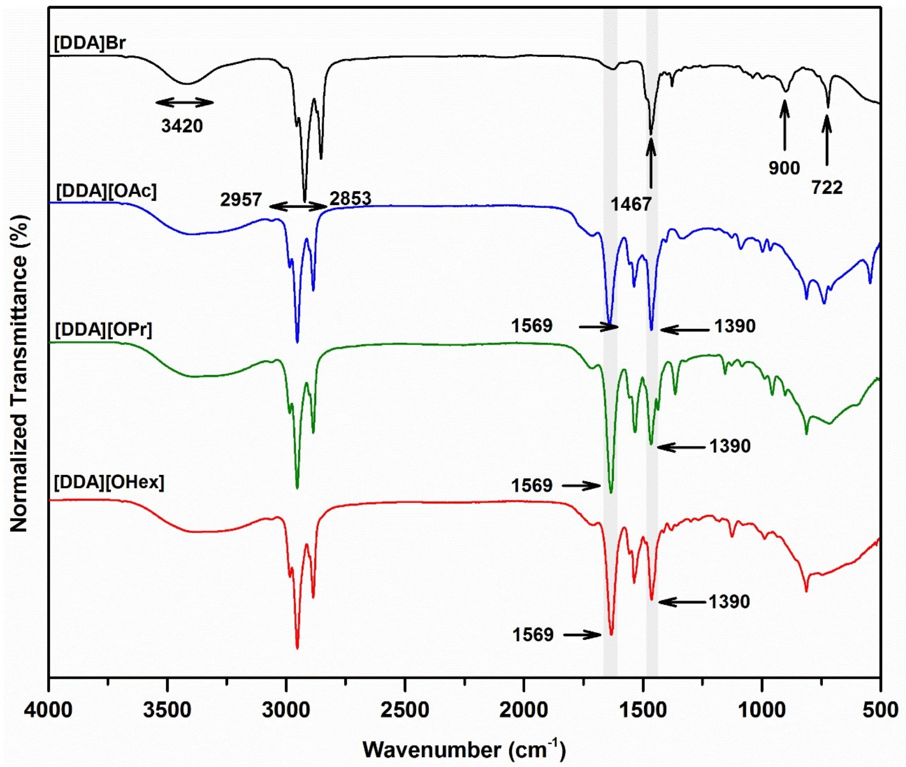

SI-Figure 14. FTIR-ATR spectra of [DDA]Br and [DDA] based-ILs.

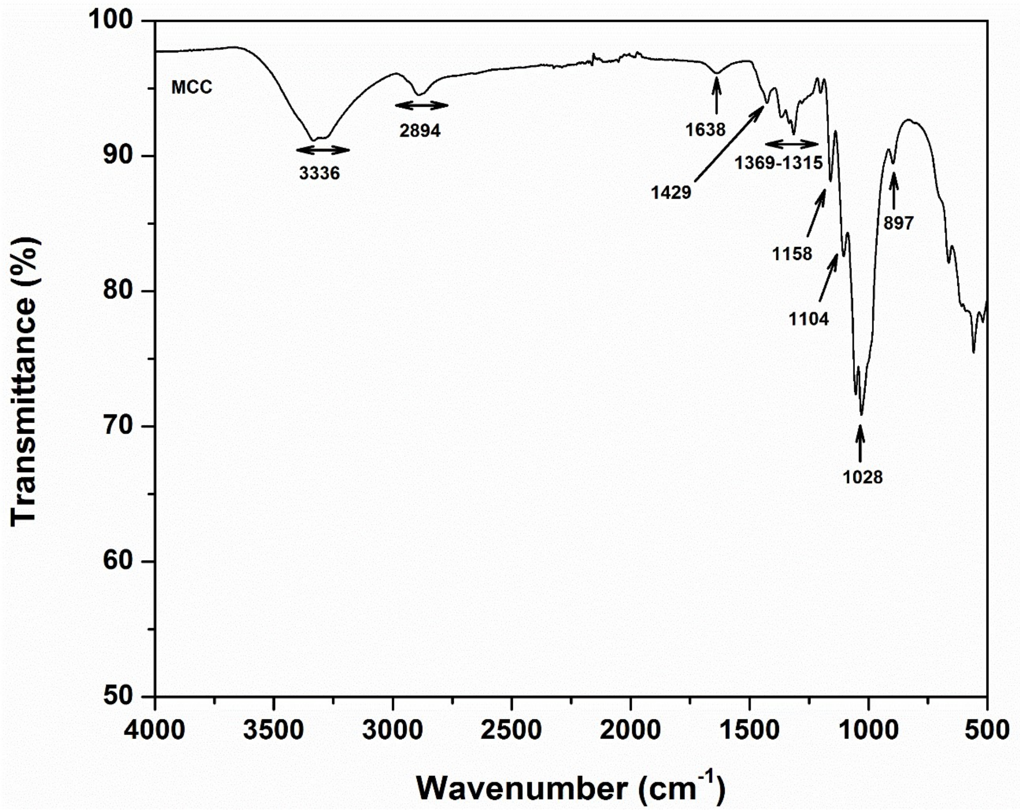

SI-Figure 15. FTIR-ATR spectra of microcrystalline (MCC).

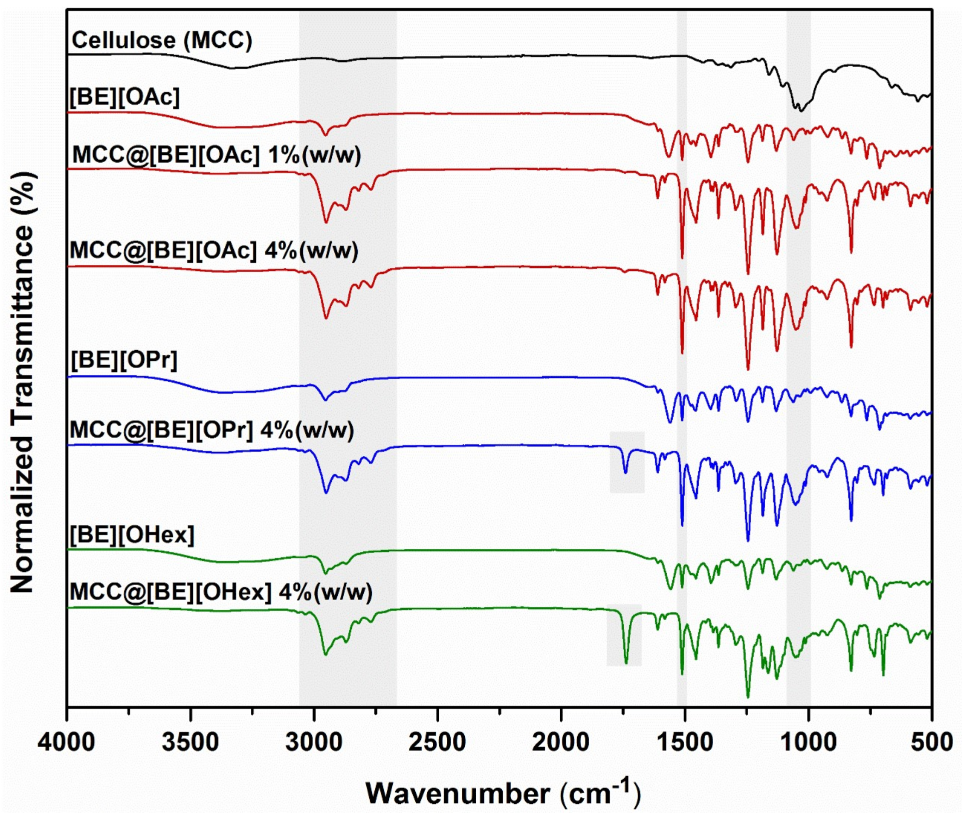

SI-Figure 16. FTIR-ATR spectra of microcrystalline cellulose (MCC) and the resulted polymeric structures prepared using [BE]-ILs as dissolution agents.

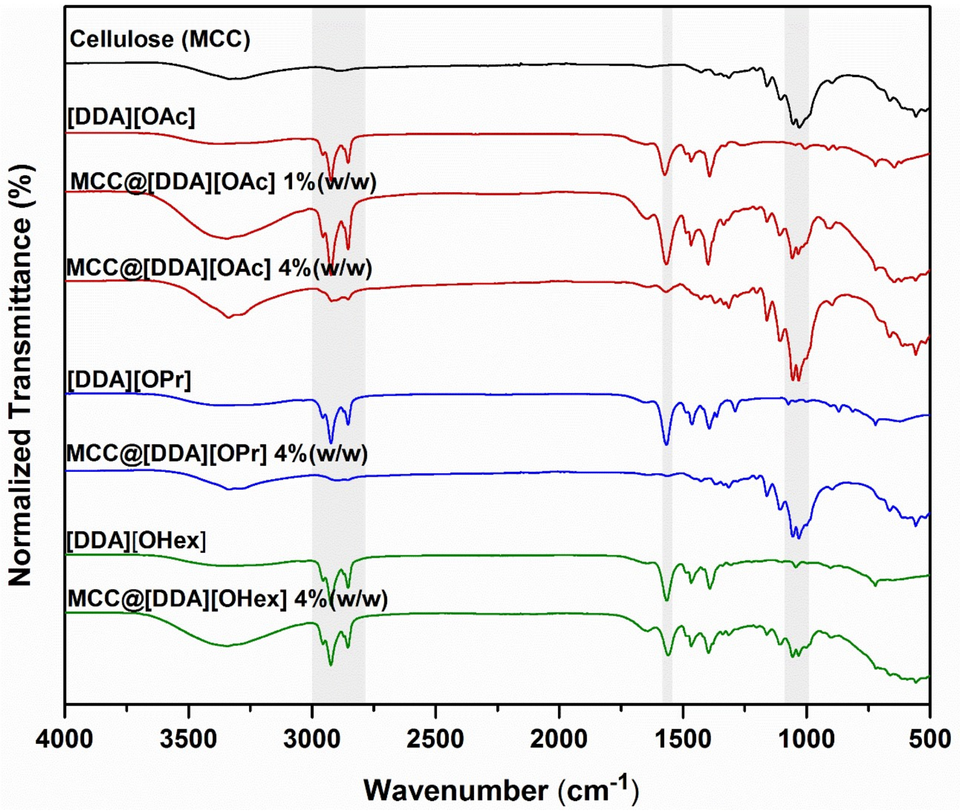

SI-Figure 17. FTIR-ATR spectra of microcrystalline cellulose (MCC) and the resulted polymeric structures prepared using [DDA]-ILs as dissolution agents.

3. Differential Scanning Calorimetry (DSC)

3.1. Ionic Liquids (ILs)

The thermal properties namely glass transition (T_g), melting (T_m), crystallization (T_c) and cold-crystallization (T_{cc}) temperatures of [BE]- and [DDA]-based ILs are summarized in table 1.

Table 1. Thermal properties: glass transition (Tg), melting (Tm), crystallization (Tc) and cold-crystallization (Tcc) temperatures as well as thermal degradation temperatures (Td,5%-onset and Td, peak) of [BE]- and [DDA]-based ILs.

IL	$DSC_{hydrated}$ [a]			DSC_{dried} [b]		
	$T_{g\text{-}mid}$(°C)	T_c/T_m(°C)	T_{cc} (°C)	$T_{g\text{-}mid}$(°C)	T_c/T_m (°C)	T_{cc} (°C)
[BE]Cl	-	-/162.4 [d]	-	-	-/-	-
[BE][OAc]	-48.1	-/-	-	-14.4	-/-	-
[BE][OPr]	-48.0	-/-	-	-14.7	-/-	-
[BE][OHex]	-52.1	-2.5/2.4	-	-29.1	-/-	-
[DDA]Br	-73.7	-/11.7; 39.5; 83.4	-21.4	-	36.8; 15.1; -2.7; -14.7/ 5.9;35.0; 68.6	-
[DDA][OAc]	-79.7	-/36.5[e]	-	-61.6	-58.0/-38.4	-
[DDA][OPr]	-78.9	-/29.4	-	-69.1	22.4/38.8	-8.9
[DDA][OHex]	-67.9	-/-2.0	-55.0; -30.8; -22.0	-76.7	6.9; -22.1/17.9; 39.0	-33.3; -3.0

[a] 1st cycle scanned at 10°C min^{-1} (hydrated state). [b] 3rd cycle scanned at 10°C min^{-1} (dried state).

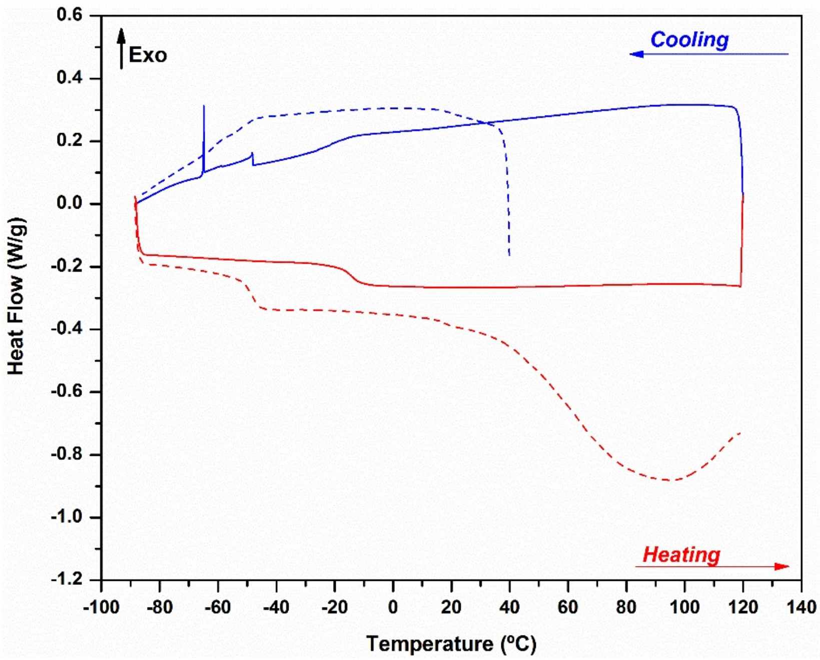

SI-Figure 18. Thermogram obtained by DSC experiment for [BE][OAc] at 10ºC min^{-1} as cooling and heating rate from -90 to 120ºC. Solid line corresponds to the first cooling and subsequently, heating runs, and dashed cooling corresponds to the third cooling and subsequently, heating runs.

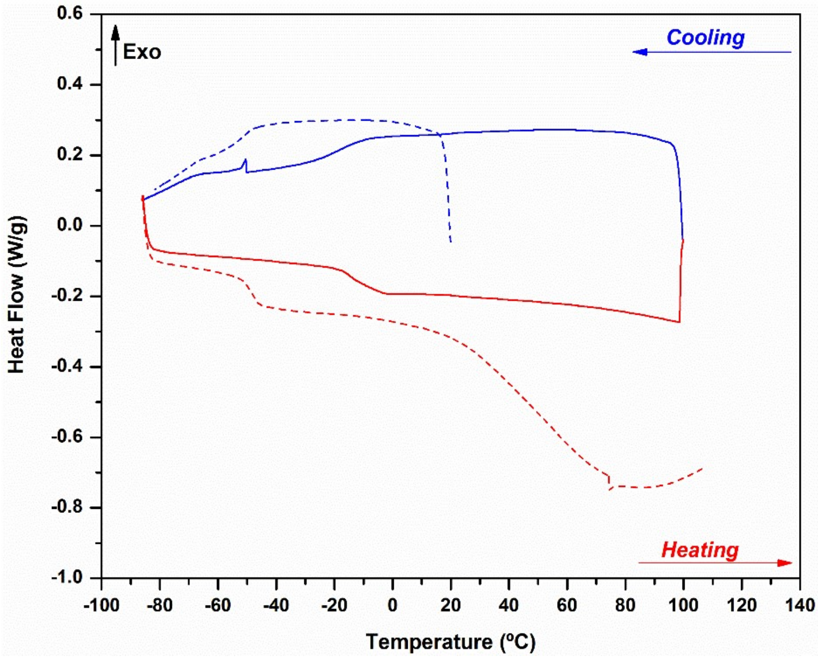

SI-Figure 19. Thermogram obtained by DSC experiment for [BE][OPr] at 10ºC min^{-1} as cooling and heating rate from -90 to 110ºC. Solid line corresponds to the first cooling and subsequently, heating runs, and dashed cooling corresponds to the third cooling and subsequently, heating runs.

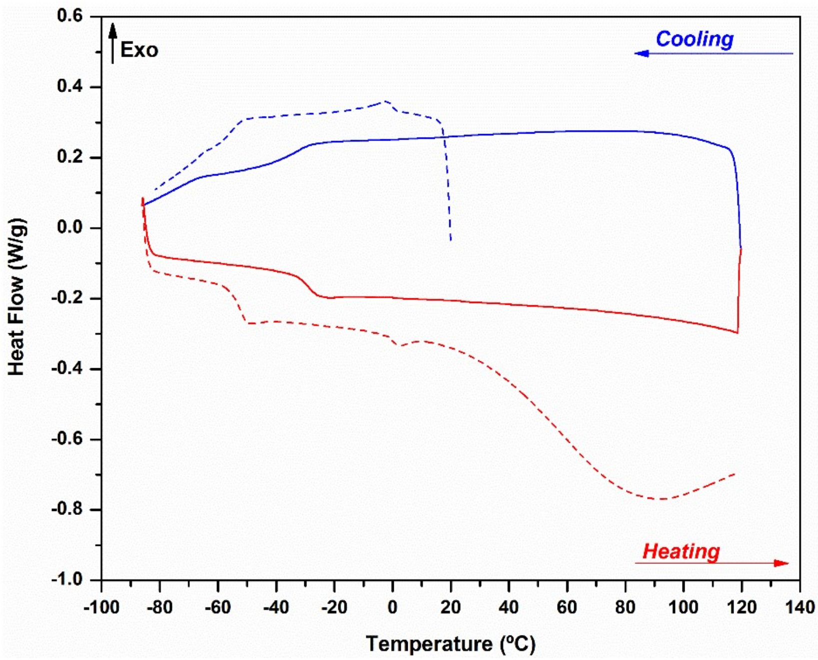

SI-Figure 20. Thermogram obtained by DSC experiment for [BE][Ohex] at 10ºC min^{-1} as cooling and heating rate from -90 to 120ºC. Solid line corresponds to the first cooling and subsequently, heating runs, and dashed cooling corresponds to the third cooling and subsequently, heating runs.

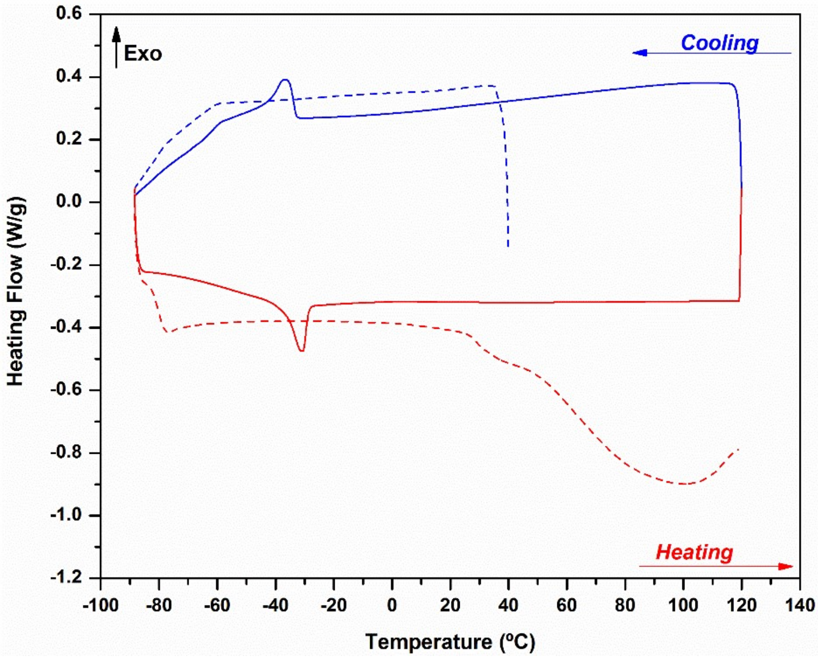

SI-Figure 21. Thermogram obtained by DSC experiment for [DDA][OAc] at 10ºC min^{-1} as cooling and heating rate from -90 to 120ºC. Solid line corresponds to the first cooling and subsequently, heating runs, and dashed cooling corresponds to the third cooling and subsequently, heating runs.

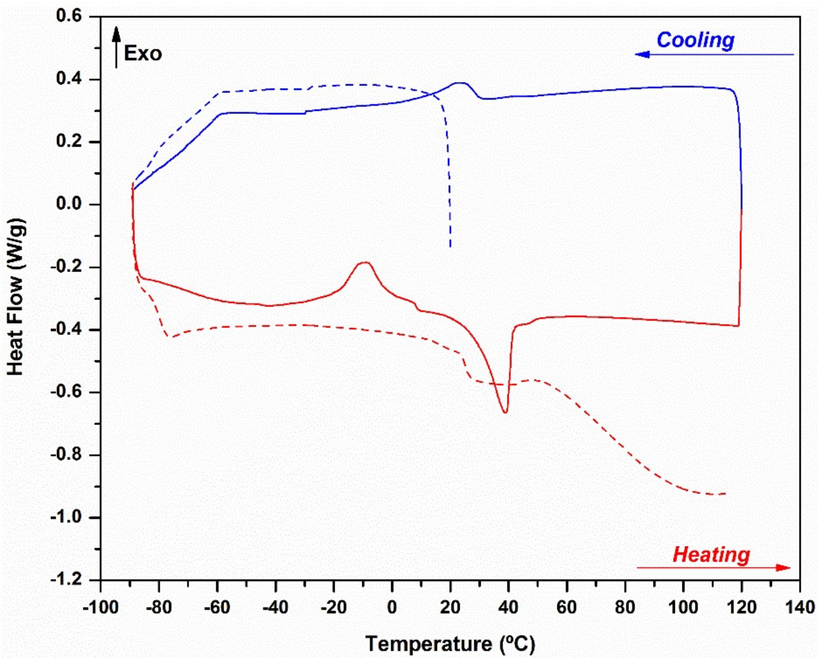

SI-Figure 22. Thermogram obtained by DSC experiment for [DDA][OPr] at 10ºC min^{-1} as cooling and heating rate from -90 to 120ºC. Solid line corresponds to the first cooling and subsequently, heating runs, and dashed cooling corresponds to the third cooling and subsequently, heating runs.

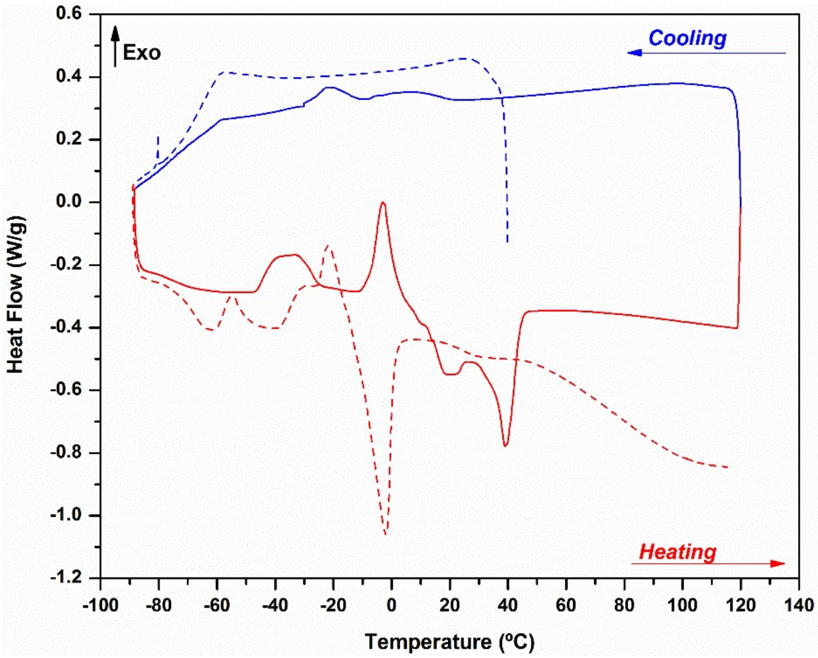

SI-Figure 23. Thermogram obtained by DSC experiment for [DDA][OHex] at 10ºC min^{-1} as cooling and heating rate from -90 to 120ºC. Solid line corresponds to the first cooling and subsequently, heating runs, and dashed cooling corresponds to the third cooling and subsequently, heating runs.

3.2. Polymeric Structures

The thermal properties namely glass transition (T_g), melting (T_m), crystallization (T_c) and cold-crystallization (T_{cc}) temperatures as well as thermal degradation temperatures ($T_{d,5\%\text{-onset}}$ and $T_{d,\,peak}$) of MCC, and the respective obtained polymeric structures are summarized in table 2.

Table 2. Thermal properties: glass transition (Tg), melting (Tm), crystallization (Tc) and cold-crystallization (Tcc) temperatures as well as thermal degradation temperatures (Td,5%-onset and Td, peak) of [BE]- and [DDA]-based ILs.

Sample	$DSC_{hydrated}$ [a]			DSC_{dried} [b]		
	$T_{g\text{-}mid}$ (°C)	T_c/T_m (°C)	T_{cc} (°C)	$T_{g\text{-}mid}$ (°C)	T_c/T_m (°C)	T_{cc} (°C)
MCC	-	-	-	-	-	-
MCC@[BE][OAc] (1% w/w)	-63.5	-	-	-64.5	-	-
MCC@[BE][OAc] (4% w/w)	-65.3	-	-	-66.0	-	-
MCC@[BE][OPr] (4% w/w)	-72.8	-	-	-73.4	-	-
MCC@[BE][OHex] (4% w/w)	-	-	-	-	-	-
MCC@[DDA][OAc] (1% w/w)	-	-	-	-	-	-
MCC@ [DDA][OAc] (4% w/w)	-	-	-	-	-	-
MCC@ [DDA][OPr] (4% w/w)	-	-	-	-	-	-
MCC@[DDA][OHex] (4% w/w)	-	-31.3/-7.3	-	-64.6	-13.6/-2.2; 39.2	4.7

[a] 1st cycle scanned at 10°C min^{-1} (hydrated state). [b] 3rd cycle scanned at 10°C min^{-1} (dried state).

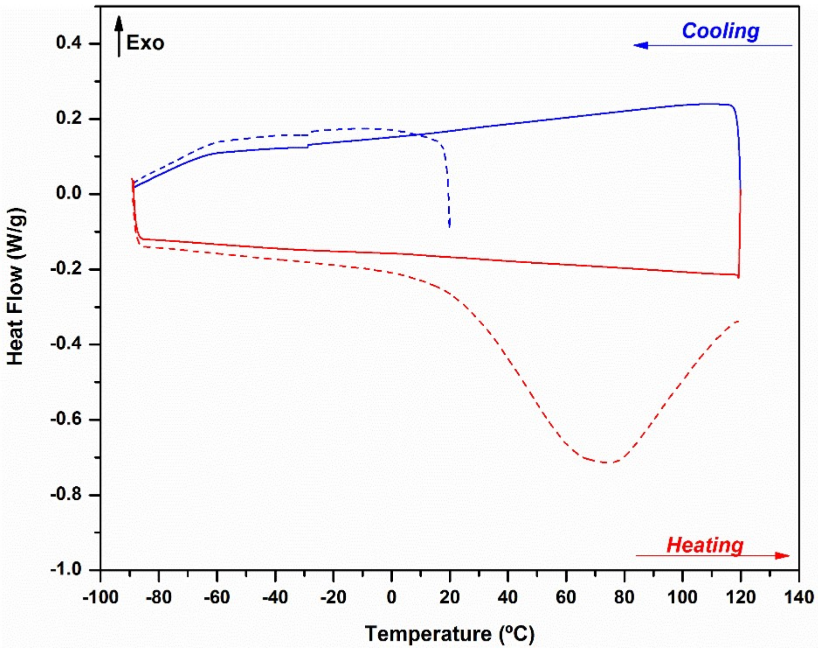

SI-Figure 24. Thermogram obtained by DSC experiment for cellulose microcrystalline (MCC) at 10ºC min^{-1} as cooling and heating rate from -90 to 120ºC. Solid line corresponds to the first cooling and subsequently, heating runs, and dashed cooling corresponds to the third cooling and subsequently, heating runs.

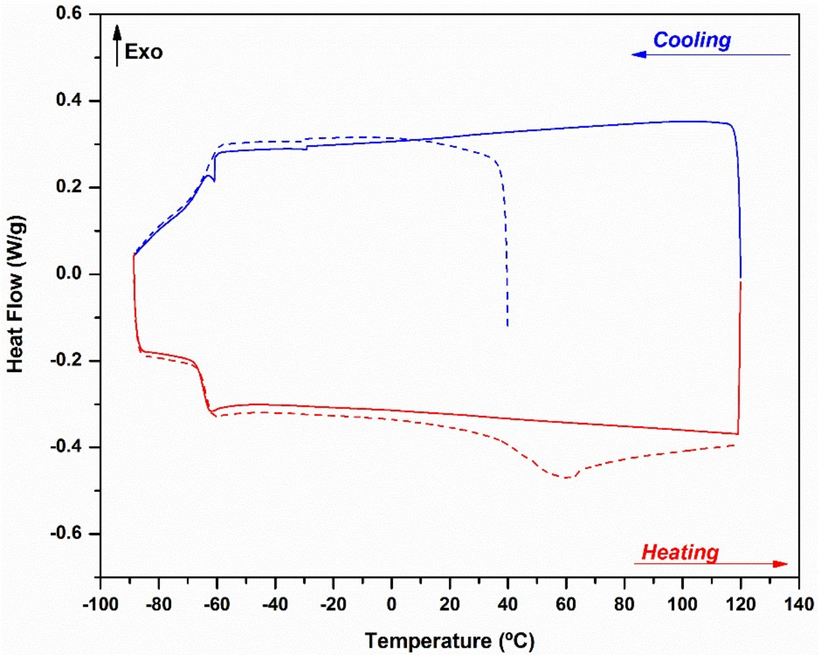

SI-Figure 25. Thermogram obtained by DSC experiment for MCC@[BE][OAc] (1% w/w) at 10ºC min^{-1} as cooling and heating rate from -90 to 120ºC. Solid line corresponds to the first cooling and subsequently, heating runs, and dashed cooling corresponds to the third cooling and subsequently, heating runs.

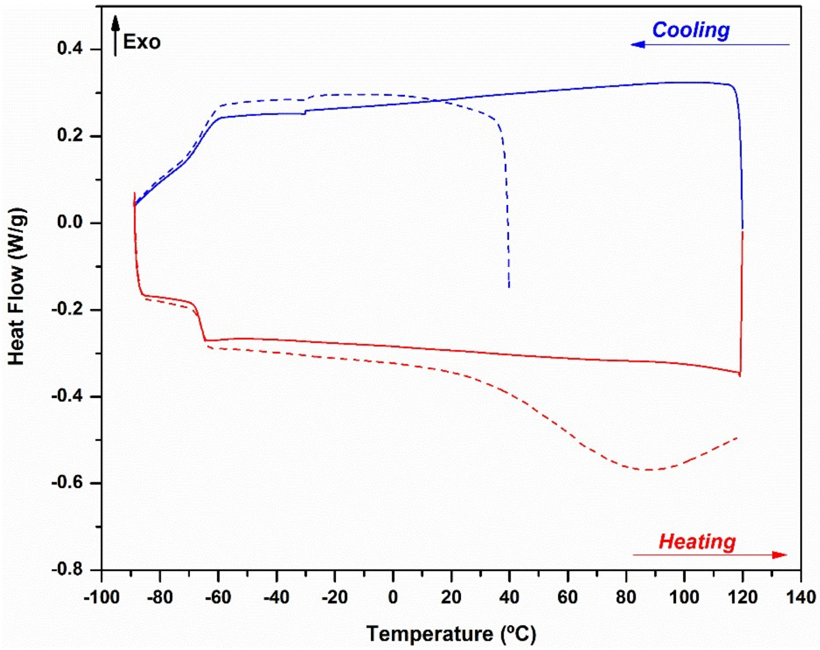

SI-Figure 26. Thermogram obtained by DSC experiment for MCC@[BE][OAc] (4% w/w) at 10ºC min^{-1} as cooling and heating rate from -90 to 120ºC. Solid line corresponds to the first cooling and subsequently, heating runs, and dashed cooling corresponds to the third cooling and subsequently, heating runs.

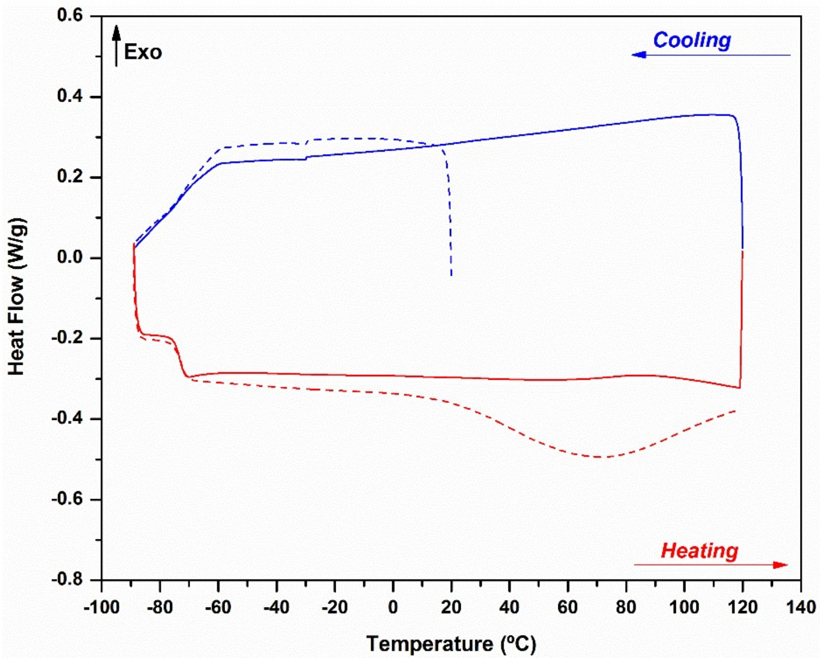

SI-Figure 27. Thermogram obtained by DSC experiment for MCC@[BE][OPr] (4% w/w) at 10ºC min^{-1} as cooling and heating rate from -90 to 120ºC. Solid line corresponds to the first cooling and subsequently, heating runs, and dashed cooling corresponds to the third cooling and subsequently, heating runs.

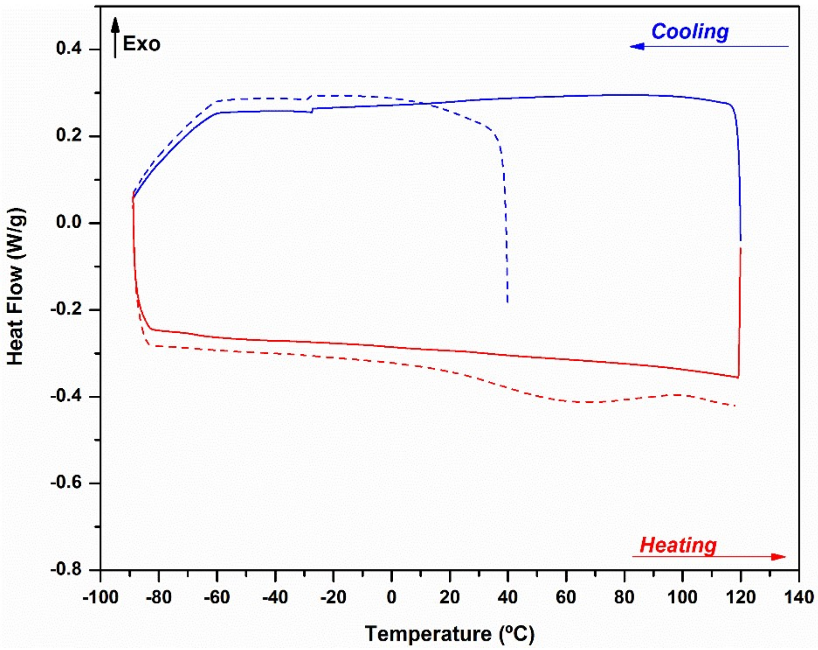

SI-Figure 28. Thermogram obtained by DSC experiment for MCC@[BE][OHex] (4% w/w) at 10ºC min^{-1} as cooling and heating rate from -90 to 120ºC. Solid line corresponds to the first cooling and subsequently, heating runs, and dashed cooling corresponds to the third cooling and subsequently, heating runs.

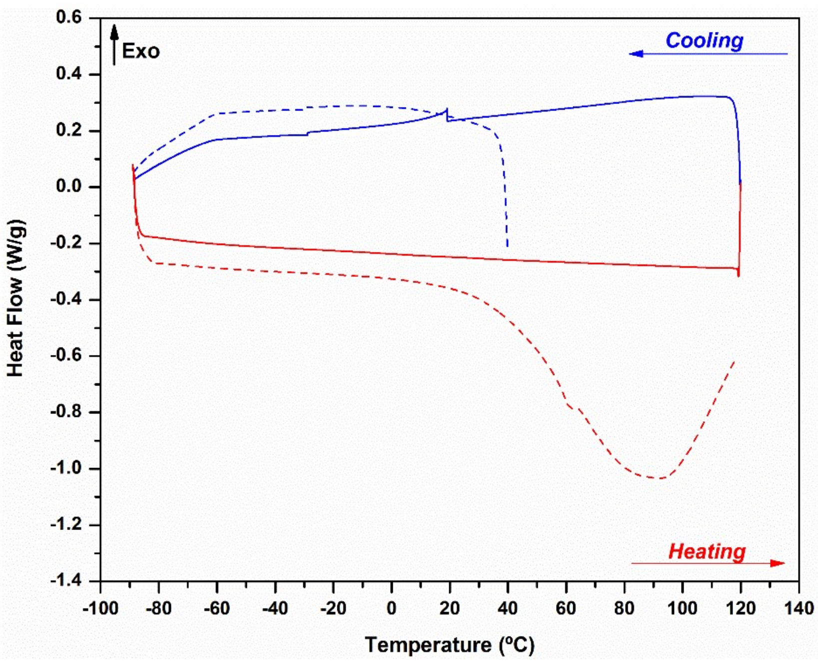

SI-Figure 29. Thermogram obtained by DSC experiment for MCC@[DDA][OAc] (1% w/w) at 10ºC min^{-1} as cooling and heating rate from -90 to 120ºC. Solid line corresponds to the first cooling and subsequently, heating runs, and dashed cooling corresponds to the third cooling and subsequently, heating runs.

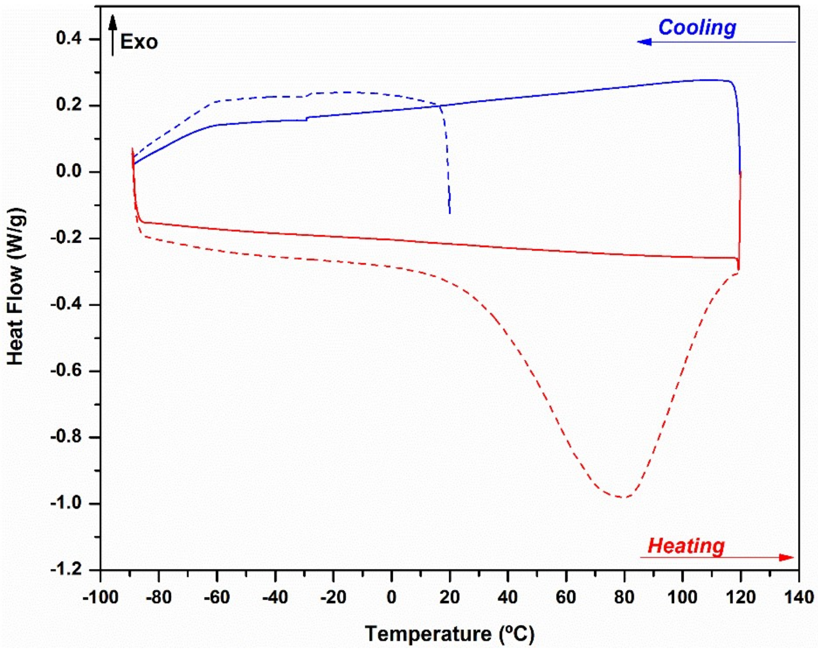

SI-Figure 30. Thermogram obtained by DSC experiment for MCC@[DDA][OAc] (4% w/w) at 10ºC min^{-1} as cooling and heating rate from -90 to 120ºC. Solid line corresponds to the first cooling and subsequently, heating runs, and dashed cooling corresponds to the third cooling and subsequently, heating runs.

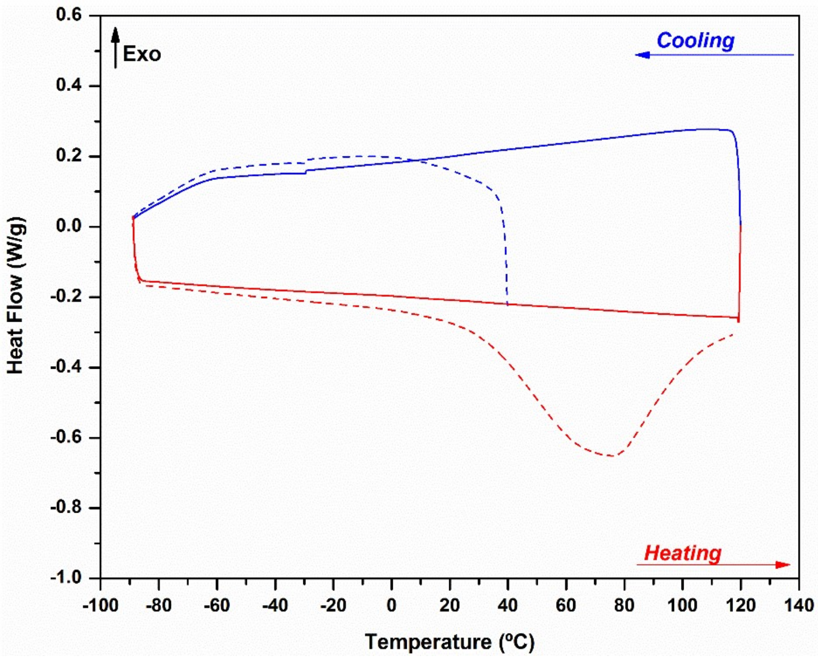

SI-Figure 31. Thermogram obtained by DSC experiment for MCC@[DDA][OPr] (4% w/w) at 10ºC min^{-1} as cooling and heating rate from -90 to 120ºC. Solid line corresponds to the first cooling and subsequently, heating runs, and dashed cooling corresponds to the third cooling and subsequently, heating runs.

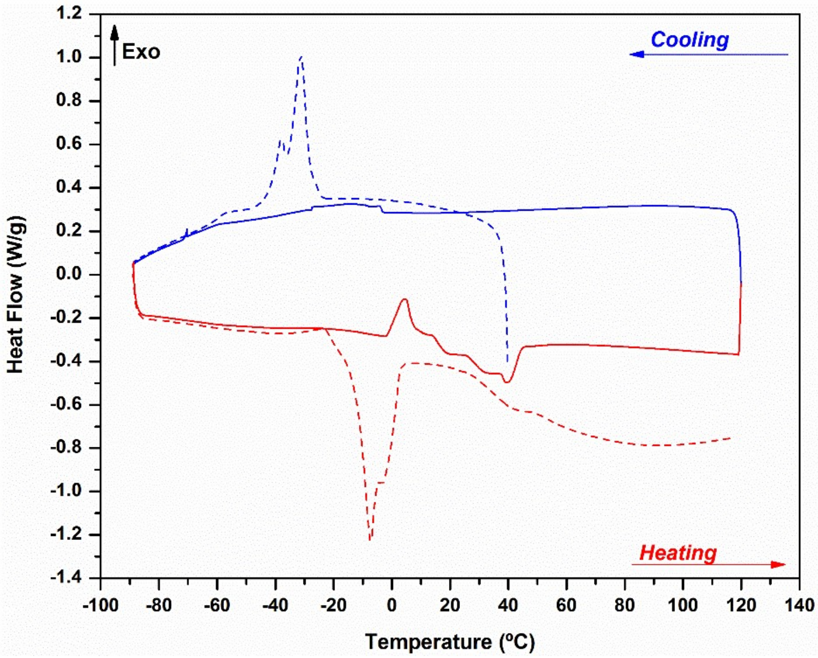

SI-Figure 32. Thermogram obtained by DSC experiment for MCC@[DDA][Ohex] (4% w/w) at 10ºC min^{-1} as cooling and heating rate from -90 to 120ºC. Solid line corresponds to the first cooling and subsequently, heating runs, and dashed cooling corresponds to the third cooling and subsequently, heating runs.

4. Thermogravimetric Analysis

Table 3. Thermal degradation temperatures ($T_{d,5\%\text{-onset}}$ and $T_{d,\ peak}$) of starting chloride and bromide salts and ionic liquids.

IL	$T_{d,5\%\text{-onset}}$ (°C) [a]	$T_{d,\ peak}$ (°C) [b]
[BE]Cl	189.0	202.0
[BE][OAc]	146.6	163.6
[BE][OPr]	128.7	163.2
[BE][OHex]	144.7	168.0
[DDA]Br	212.1	247.3
[DDA][OAc]	128.6	183.4
[DDA][OPr]	172.6	184.8
[DDA][OHex]	167.1	187.0

[a] $T_{d,5\%\text{-onset}}$ – onset temperature where the sample lost 5% of initial weight; [b] $T_{d,peak}$ – temperature associated with the first step of the mass loss process, which were taken as the minimum of the derivative of thermogravimetric curves (DTGA) was determined from simultaneous TGA-DSC experiments acquired from 25°C to 500°C at 10°C min^{-1} under argon atmosphere.

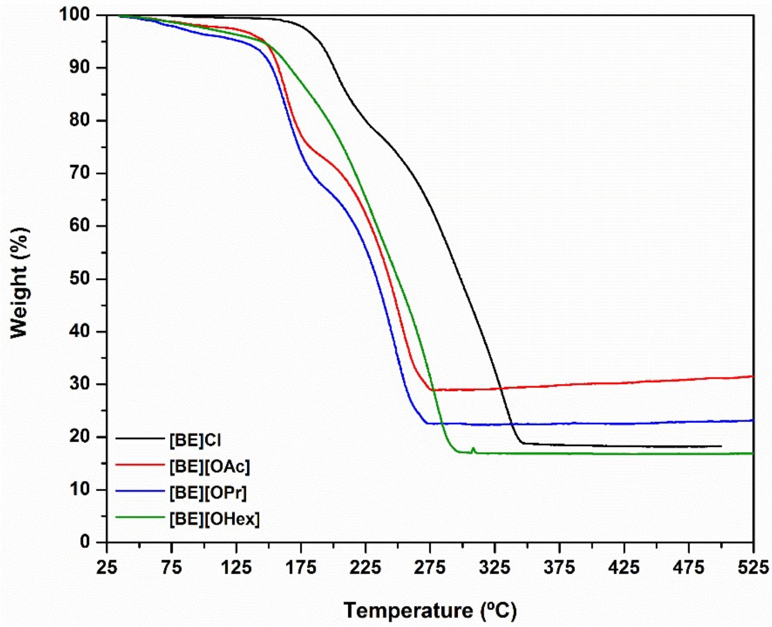

SI-Figure 33. Thermogravimetric curve obtained by Simultaneously TGA-DSC experiments for [BE]Cl and [BE] based-ILs at a heating rate of 10ºC min^{-1} from 25ºC to 500-600ºC under argon atmosphere.

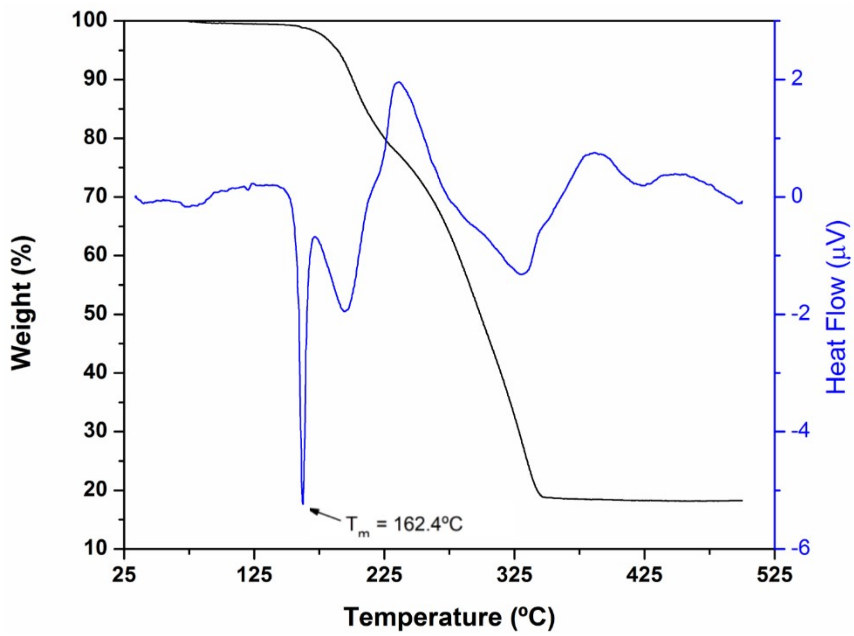

SI-Figure 34. Thermogravimetric curve and respective heat flow thermogram obtained by Simultaneously TGA-DSC experiments for [BE]Cl at a heating rate of 10ºC min^{-1} from 25ºC to 500-600ºC under argon atmosphere.

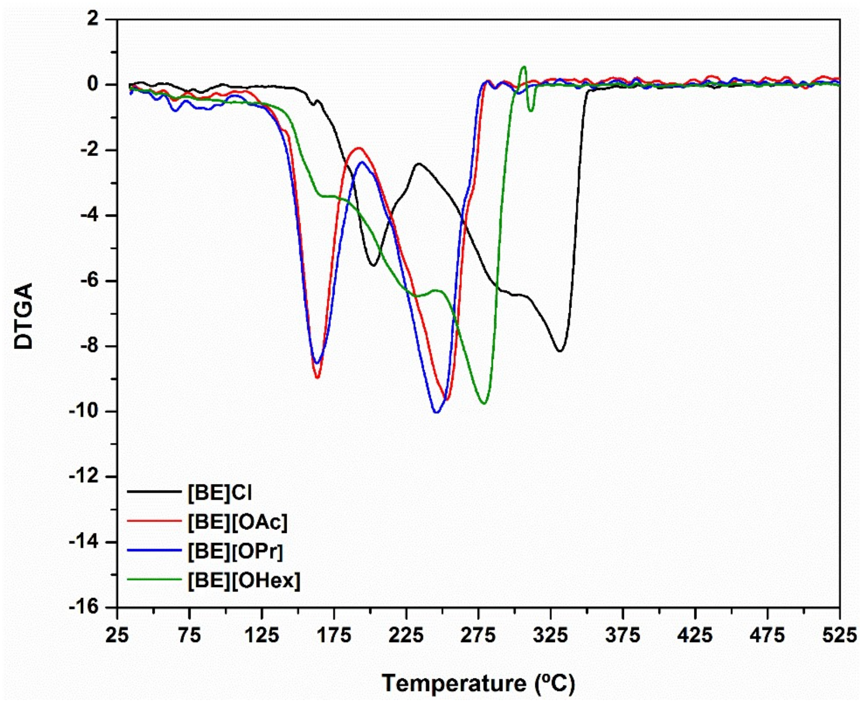

SI-Figure 35. Differential thermogravimetry curve calculated as the first derivative of the weight with respect to temperature for [BE]Cl and [BE] based-ILs at a heating rate of 10ºC min^{-1} from 25ºC to 500-600ºC under argon atmosphere.

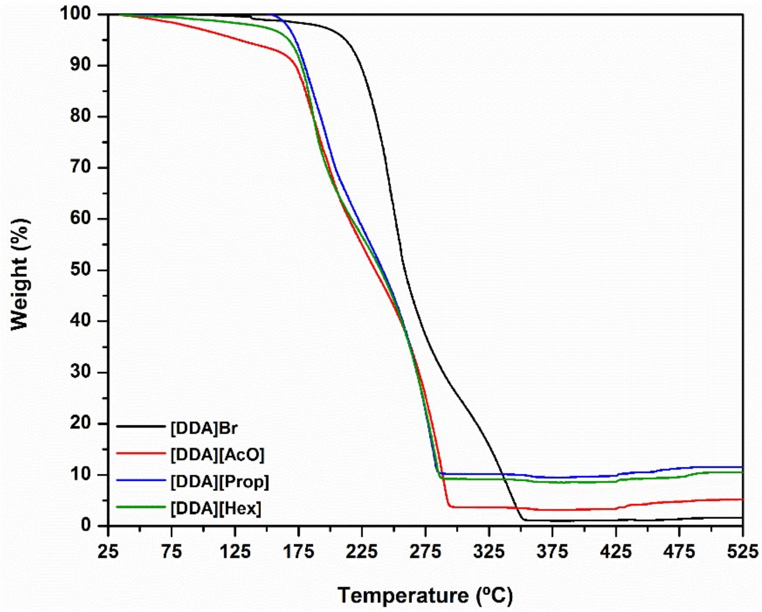

SI-Figure 36. Thermogravimetric curve obtained by Simultaneously TGA-DSC experiments for [DDA]Br and [DDA] based-ILs at a heating rate of 10ºC min^{-1} from 25ºC to 600ºC under argon atmosphere.

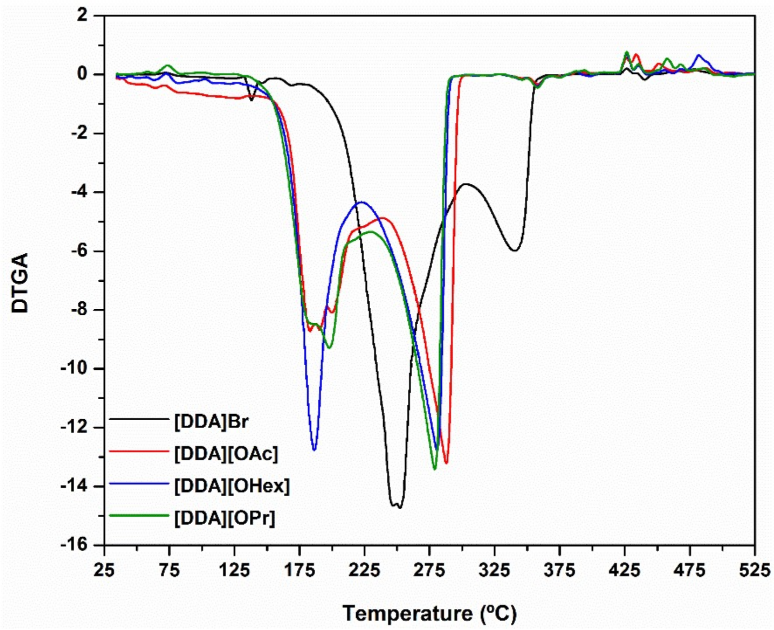

SI-Figure 37. Differential thermogravimetry curve calculated as the first derivative of the weight with respect to temperature for [DDA]Br and [DDA] based-ILs at a heating rate of 10ºC min^{-1} from 25ºC to 600ºC under argon atmosphere.

Table 4. Thermal degradation temperatures ($T_{d,5\%\text{-onset}}$ and $T_{d,\ peak}$) of MCC and respective obtained polymeric structures.

Sample	$T_{d,5\%\text{-onset}}$ (°C) [a]	$T_{d,\ peak}$ (°C) [b]
MCC	289.86	331.90
MCC@[BE][OAc] (1% w/w)	217.32	307.86
MCC@[BE][OAc] (4% w/w)	210.77	306.08
MCC@[BE][OPr] (4 % w/w)	160.45	298.85
MCC@[BE][OHex] (4% w/w)	168.95	239.33
MCC@[DDA][OAc] (1 % w/w)	94.74	209.96
MCC@[DDA][OAc] (4 % w/w)	194.61	229.26
MCC@ [DDA][OPr] (4 % w/w)	192.19	228.28
MCC@[DDA][OHex] (4% w/w)	170.67	202.65

[a] Td,5%-onset – onset temperature where the sample lost 5% of initial weight; [b] Td,peak – temperature associated with the first step of the mass loss process, which were taken as the minimum of the derivative of thermogravimetric curves (DTGA) was determined from simultaneous TGA-DSC experiments acquired from 25°C to 500°C at 10°C min-1 under argon atmosphere.

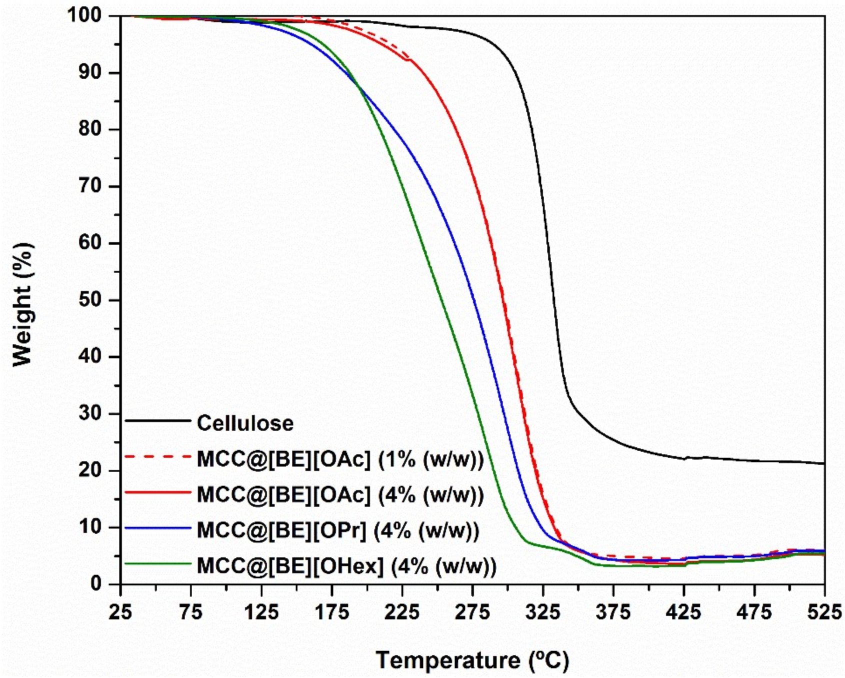

SI-Figure 38. Thermogravimetric curve obtained by Simultaneously TGA-DSC experiments for MCC and the polymeric structures obtained using [BE] based-ILs as dissolution agent at a heating rate of 10ºC min^{-1} from 25ºC to 600ºC under argon atmosphere.

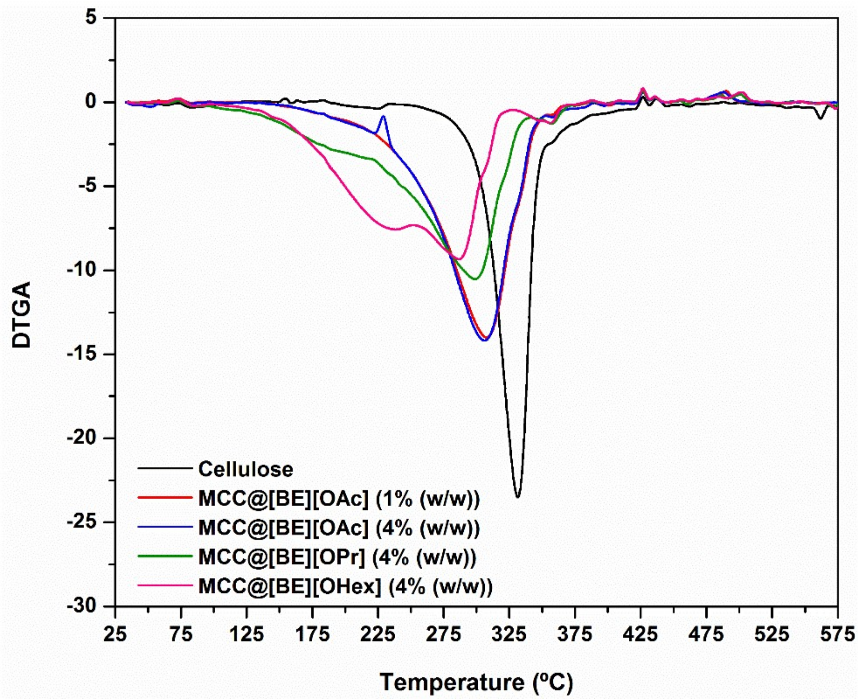

SI-Figure 39. Differential thermogravimetry curve calculated as the first derivative of the weight with respect to temperature Thermogravimetric curve obtained by Simultaneously TGA-DSC experiments for MCC and the polymeric structures obtained using [BE] based-ILs as dissolution agent at a heating rate of 10ºC min^{-1} from 25ºC to 600ºC under argon atmosphere.

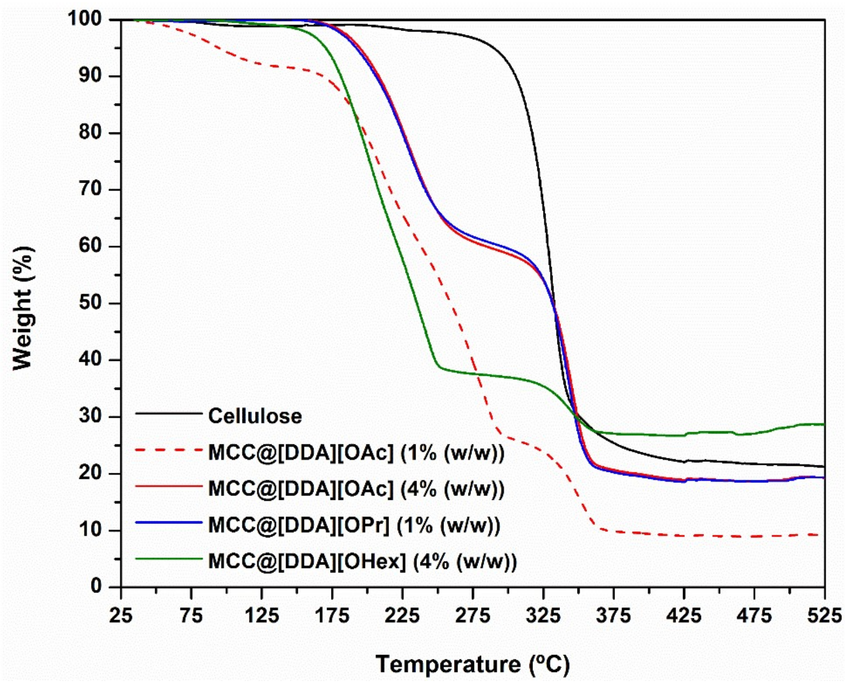

SI-Figure 40. Thermogravimetric curve obtained by Simultaneously TGA-DSC experiments for MCC and polymeric structures obtained using [DDA] based-ILs as dissolution agent at a heating rate of 10ºC min^{-1} from 25ºC to 600ºC under argon atmosphere.

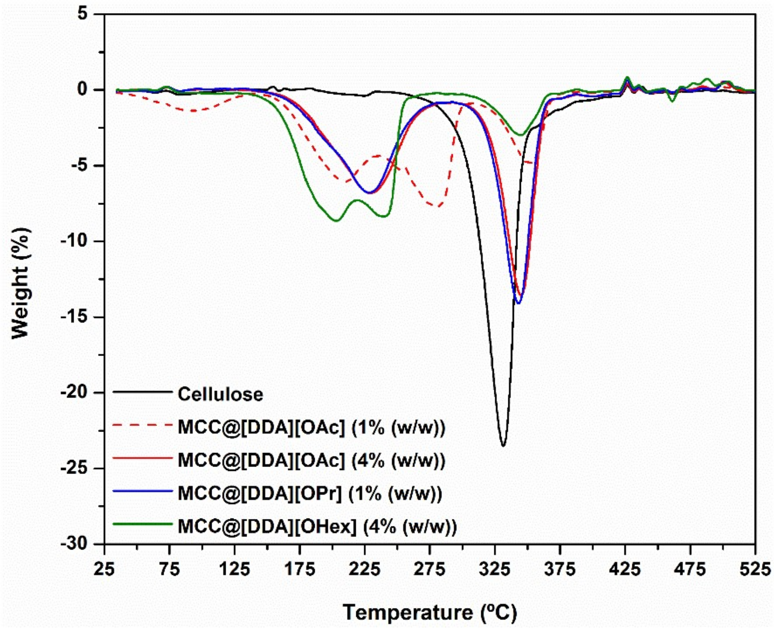

SI-Figure 41. Differential thermogravimetry curve calculated as the first derivative of the weight with respect to temperature Thermogravimetric curve obtained by Simultaneously TGA-DSC experiments for MCC and the polymeric structures obtained using [DDA] based-ILs as dissolution agent at a heating rate of 10ºC min^{-1} from 25ºC to 600ºC under argon atmosphere.

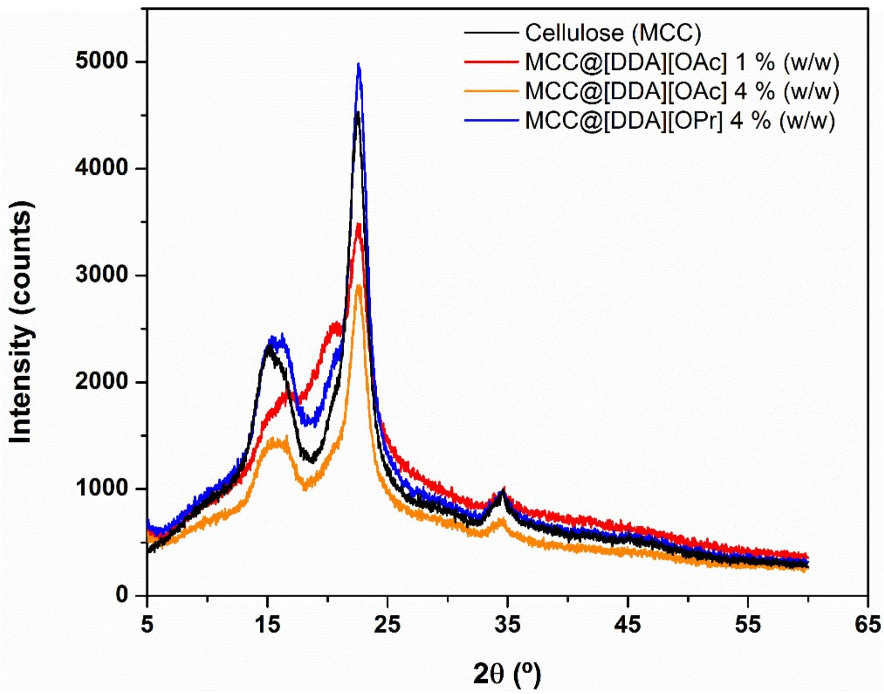

SI-Figure 42. X-ray diffraction spectra of MCC and the obtained films.